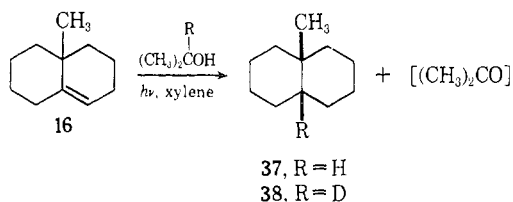


of pinacol and free-radical addition products of acetone and octalin **15**<sup>30</sup> shows that isopropyl alcohol functions as the reducing agent in this reaction. In 2-deuterio-2-propanol the photosensitized reduction afforded *cis*-9-methyl-10-deuteriodecalin (**38**) as the sole reduction product.<sup>10</sup> Since deuterium adds to the more substituted position of octalin **16**, a mechanism involving deuterium atom abstraction<sup>31</sup> from the alcohol appears untenable as this pathway would lead to deuterium incorporation at the secondary position. However, the observed results can be accommodated by an ionic pathway involving hydride transfer from isopropyl alcohol to the C-10 cation derived from octalin **16**.

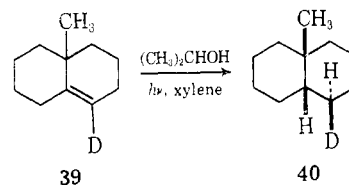


The stereochemistry of the hydrogenation reaction was ascertained through irradiation of the deuterated octalin **39** in isopropyl alcohol-xylene. The resulting *cis*-decalin **40** was identified by comparison with an authentic sample synthesized independently.<sup>26</sup> Thus,

(30) Cf. J. S. Bradshaw, *J. Org. Chem.*, **31**, 237 (1966).

(31) Cf. R. R. Sauer, W. Schinski, and M. M. Mason, *Tetrahedron Letters*, 4763 (1967).

protonation of octalin **16** *trans* to the angular methyl grouping appears to be highly preferred in both the photochemical hydration and hydrogenation reactions.



The stereochemical results to date on photosensitized ionic additions to cyclohexene double bonds seem best accommodated by the chair form of a *trans*-cyclohexene intermediate. Protonation of such an intermediate from the outside face must necessarily lead to an equatorially oriented C-H bond in the chair form of the resulting cyclohexyl cation. This cation, or a related ion pair, then reacts with the nucleophilic portion of the addend either by elimination or by addition, depending upon the steric requirements of the nucleophile and the steric environment of the cation.

*I am deeply grateful to my collaborators, R. D. Carroll, H. Faubl, A. Greene, A. R. Hochstetler, and M. Wurth, for their dedicated efforts in the pursuit and interpretation of the experimental data which forms the basis of this report. The continued cooperation and interest of Dr. P. J. Kropp has also been of great value. Finally financial assistance from the National Science Foundation, the Hoffmann-La Roche Foundation, and the Alfred P. Sloan Foundation which made this research possible is gratefully acknowledged.*

## High-Pressure Mössbauer Resonance Studies with Iron-57<sup>1</sup>

H. G. DRICKAMER

*Department of Chemistry and Chemical Engineering and Materials Research Laboratory, University of Illinois, Urbana, Illinois*

R. W. VAUGHAN

*Physics Division, Jet Propulsion Laboratory, Pasadena, California*

A. R. CHAMPION

*Sandia Corporation, Albuquerque, New Mexico*

*Received July 29, 1968*

The Mössbauer effect is a useful tool for investigating a number of aspects of chemistry and physics, since it allows one to compare very accurately the energy of specific nuclear transitions. The energy of a nuclear transition is slightly modified by surrounding electrons, and by measuring these energy modifications it is possible to deduce information about the chemical nature of the environment. In this paper we discuss the effect of pressure on compounds of iron.

The principles of Mössbauer resonance have been

(1) This work supported in part by the U. S. Atomic Energy Commission under Contract AT(11-1)-1198.

thoroughly discussed,<sup>2</sup> and will be reviewed only briefly here. The emission or absorption of a  $\gamma$  ray by the nucleus of a free atom involves Doppler broadening and recoil processes. The basic discovery of Mössbauer was that, by fixing the atom in a solid where the momentum is quantized and the motion limited to vibrational modes, these effects might be eliminated. If the lowest allowed quantum of lattice vibrational energy (lowest phonon energy) is large compared with

(2) (a) H. Frauenfelder, "The Mössbauer Effect," W. A. Benjamin, Inc., New York, N. Y., 1963; (b) G. K. Wertheim, "Mössbauer Effect: Theory and Applications," Academic Press, New York, N. Y., 1964.

the classical recoil energy for absorption or emission, a large fraction of recoilless decays is possible, and, as the net velocity of a vibrating system is zero, there will be no Doppler broadening. Thus the width of the peak will be established by the uncertainty principle plus instrumental broadening and relaxation effects. Energy changes of the order of  $10^{-5}$  cal ( $\sim 10^{-9}$  eV) are measurable.

There is a variety of Mössbauer isotopes and a number of properties which can be studied. We shall confine ourselves to a discussion of the 14.4-keV transition in  $\text{Fe}^{57}$  and to two kinds of readout: the isomer shift and the quadrupole splitting. As mentioned above, nuclear states are slightly perturbed by electronic wave functions having nonzero amplitude at the nuclear site (*s* electrons), so a source and absorber with different electronic configurations are not in resonance. By moving the source with respect to the absorber, and thus effecting a Doppler shift on the energy of the emitted  $\gamma$  ray to compensate for this energy difference (called the isomer shift), one can establish resonance. A Mössbauer spectrometer is, then, a device for producing and measuring accurately the velocities necessary to obtain resonance between source and absorber in different environments. In this work energy differences are reported in millimeters per second relative to metallic (body-centered cubic) iron at 1 atm. The apparatus for high-pressure Mössbauer studies is described in the literature.<sup>3,4</sup>

In iron compounds the 1s and 2s electronic wave functions have large amplitudes at the nucleus but are shielded from the environment. (The excellent correlation that Erickson<sup>5</sup> obtains between isomer shift and chemical properties, for example, indicates the controlling effect of the chemical environment, *i.e.*, the 3s and 4s electrons.) If there are 4s electrons present, they interact strongly with the surroundings. The 3s electrons do not interact directly, but they have their radial maximum at about the same point as the 3d electrons, and these do interact with the ligands. Changes in the 3d wave functions are thus reflected in changes in shielding of the 3s electrons.

The difference in isomer shift between source and absorber is given by eq 1. For iron  $\alpha = 3.52 \times 10^{10}$

$$\Delta\epsilon = \alpha[\psi_s^2(0) - \psi_A^2(0)] \quad (1)$$

$R\Delta R$ , where  $\Delta R$  is the difference of the radius of the nucleus in the ground and excited states. The evaluation of  $\alpha$  experimentally and theoretically is a subject of controversy which will engage us peripherally.

The nuclear levels can also interact with an electric field gradient at the nucleus. In iron the excited state of spin  $3/2$  splits and two peaks are observed. An electric field gradient can arise from an aspherical

distribution of electrons in the 3d shell ( $q_{\text{val}}$ ) or from a less than cubic distribution of the ligands ( $q_{\text{lat}}$ ). Because of the short range of quadrupolar forces, where the former effect is present, it dominates.

There are other readouts, such as the magnitude of a magnetic field and the fraction of recoilless decays which give useful information, but these will not be discussed here.

As an aid in discussing the Mössbauer results it is useful to review briefly some effects of pressure on optical spectra which are presented in detail elsewhere.<sup>6,7</sup> The free ion has a fivefold-degenerate 3d shell. The difference in energy between the ground and excited states can be expressed in terms of the Racah parameters, *A*, *B*, and *C*, which measure the repulsion among the 3d electrons. In a crystal field the degeneracy is partially removed. (Octahedral symmetry is used here as an example. Results for other symmetries are similar. Reference to the molecular orbital diagram on p 103 of Ballhausen and Gray<sup>8</sup> may be helpful.) There is a triply degenerate level,  $t_{2g}$ , and a doubly degenerate level,  $e_g$ , separated by an energy,  $10Dq$ , which measures the crystal field. Optical transitions of moderate intensity are observed which measure  $10Dq$ , the Racah parameters *B* and *C*, or combinations of these. With pressure, the crystal field increases by about 10–15% in 100 kbars. The Racah parameters decrease by 7–10% in the same range, which can best be explained in terms of a spreading of the 3d orbitals due to increased interaction with the ligands as pressure increases.

There are also very intense allowed transitions in the near ultraviolet (3–5 eV) with tails that extend through the visible and even into the infrared. These represent charge transfer from ligand nonbonding to metal antibonding levels ( $t_{2u} \rightarrow t_{2g}$ ). These peaks shift to lower energy by 0.5 to 1 eV in 100 kbars. The major cause of the red shift is probably the spreading of the 3d orbitals mentioned above, which could easily lower the metal levels *vis-à-vis* the ligands by this amount. Increased  $\pi$  bonding of the  $t_{2g}$  orbital with ligand  $\pi^*$  levels would also stabilize the  $t_{2g}$  level. Lewis<sup>9</sup> has shown that this is a factor, but not the major one.

Finally, there is more than one way to arrange the electrons in the 3d levels. Hund's rule demands maximum multiplicity. In this case, ferric ion, with five 3d electrons, exhibits spherical symmetry and quadrupole splitting only due to the ligand field ( $q_{\text{lat}}$ ). The usual range is from 0.3 to 0.6 mm/sec. The extra electron on the high-spin ferrous ion usually guarantees an aspherical 3d shell and large quadrupole splittings

(6) H. G. Drickamer in "Solids under Pressure," W. Paul and D. Warschauer, Ed., McGraw-Hill Book Co., Inc., New York, N. Y., 1963.

(7) H. G. Drickamer in "Solid State Physics," F. Seitz and D. Turnbull, Ed., Academic Press, New York, N. Y., 1965.

(8) C. J. Ballhausen and H. B. Gray, "Molecular Orbital Theory," W. A. Benjamin, New York, N. Y., 1965.

(9) G. K. Lewis and H. G. Drickamer, *Proc. Natl. Acad. Sci. U. S.*, **61**, 414 (1968).

(3) D. Pipkörn, C. K. Edge, P. Debrunner, G. dePasquali, H. G. Drickamer, and H. Frauenfelder, *Phys. Rev.*, **135**, A1604 (1964).

(4) P. Debrunner, R. W. Vaughan, A. R. Champion, J. Cohen, J. A. Moyzis, and H. G. Drickamer, *Rev. Sci. Instr.*, **37**, 1310 (1966).

(5) N. E. Erickson in "The Mössbauer Effect and its Application in Chemistry," C. Seidel and R. Herber, Ed., *Advances in Chemistry Series*, No. 68, American Chemistry Society, Washington, D. C., 1967.

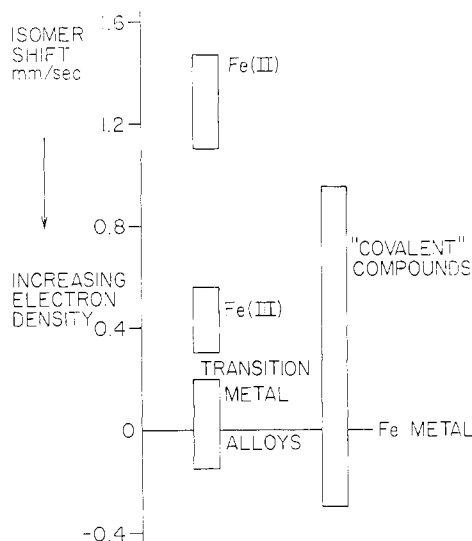


Figure 1. Ranges of isomer shift for iron.

(2–3 mm/sec). On the other hand, low-spin ferrous ion shows very small quadrupole splitting and low-spin ferric somewhat larger.

In our discussion we include two general topics: the effect of pressure on the isomer shift and the oxidation state of iron as a function of pressure, and two cases where Mössbauer resonance has revealed information on specific systems, ferrocene and  $\alpha$ - $\text{Fe}_2\text{O}_3$ .

### Isomer Shifts

It should be understood that the interpretation of the effects of chemical environment and pressure on the isomer shift is an open question. We introduce it here in part to encourage more work, both experimental and theoretical, and we express opinions which are certainly subject to possible revision.

Figure 1 shows typical ranges of isomer shift for iron in various environments (by convention, the smaller the isomer shift, the larger the electron density). There are several salient features. Iron as a dilute solute in transition metals exhibits a modest range (0.4–0.5 mm/sec) of isomer shifts considering that the solvents have from one to nine 3d electrons. Evidently the 3d electrons of iron are not totally integrated into the solvent 3d band. High-spin ferrous compounds lie in a relatively small range at very low electron density because of their nominal  $3d^6 4s^0$  configuration. High-spin ferric systems lie at considerably higher electron density with a modest range of isomer shifts quite distinct from those of ferrous ions. The compounds covered include fluorides, chlorides, bromides, sulfates, phosphates, acetates, oxalates, citrates, thiocyanates, etc. Since the ferric ion is usually assumed to be more covalent than the ferrous, the small range of isomer shifts exhibited is of interest for the later discussion. The final classification in Figure 1, "covalent," is ambiguous, but there are certainly molecules such as ferrocene or the ferro- and ferricyanides which exhibit a high degree of electron sharing, and crystals like  $\text{FeS}_2$ ,  $\text{FeSe}_2$ ,  $\text{FeTe}_2$ ,  $\text{FeP}$ ,  $\text{FeAs}_2$ ,

etc., which have no easily describable valence. As one might expect, these materials show a large range of isomer shifts.

Ingalls<sup>10</sup> found empirically a linear correlation between the maximum of the 3d radial wave function squared and the 3s density at the nucleus using Hartree-Fock free ion wave functions. A variational calculation performed to determine the effect of change in shape of 3d orbitals, going from the free ion to the metal, on 3s density at the nucleus indicates that Ingalls' correlation is still valid for the band functions, some of which have large electron densities in the tail of the orbital. Thus, in the interpretation of the isomer shift in terms of covalency, one must consider that the isomer shift is not necessarily sensitive to electron density located between the iron ion and the ligand, a normal criterion for covalency, but only to the associated change of 3d density on the ion.

In Figure 2 are plotted the isomer shifts of several high-spin  $\text{Fe(II)}$  and  $\text{Fe(III)}$  compounds as a function of pressure.<sup>9,11–13</sup> Almost all "ionic" compounds studied fall within the limits shown. Several facts are evident. For all compounds there is an increase in electron density with increasing pressure. The ferrous compounds show slightly more change than the ferric, although there is no consistent difference in compressibility. The change for ferrous compounds is 10–12% of the over-all ferrous–ferric difference in 150 kbars—a nontrivial effect. The rate of change with pressure drops off more rapidly than  $\Delta V/V$  for most ionic compounds. Figure 3 is a corresponding plot at double scale for relatively covalent compounds. Pyrites, ferrocene, and  $\text{K}_4\text{Fe(CN)}_6$  all show large changes in isomer shift, although pyrite is quite incompressible<sup>14</sup> and the Fe–C bonds in ferrocene and ferrocyanide are surely not very compressible. The acetylacetonate is apparently rather covalent, although it is high spin. It exhibits a decrease in electron density at low pressure with a reversal at high pressure.

There are two factors which would change the electron density at the nucleus with compression: (1) changes in orbital occupation (these could be either transfer of electrons to or from the 4s levels, or transfer to, from, or among the 3d levels, changing the shielding of the 3s electrons); (2) distortion of the wave functions—either compression of the s electrons or the spreading of the 3d electrons mentioned earlier. The first factor undoubtedly is important in the case of the "covalent" compounds of Figure 3. We do not believe it is significant for the systems of Figure 2.

There are two basically different theoretical approaches to the isomer shift, both attempts to evaluate

(10) R. L. Ingalls, *Phys. Rev.*, **155**, 157 (1967).

(11) A. R. Champion, R. W. Vaughan, and H. G. Drickamer, *J. Chem. Phys.*, **47**, 2583 (1967).

(12) A. R. Champion and H. G. Drickamer, *ibid.*, **47**, 2591 (1967).

(13) A. R. Champion and H. G. Drickamer, *Proc. Natl. Acad. Sci. U. S. A.*, **58**, 876 (1967).

(14) R. L. Clendenen and H. G. Drickamer, *J. Chem. Phys.*, **44**, 4223 (1966).

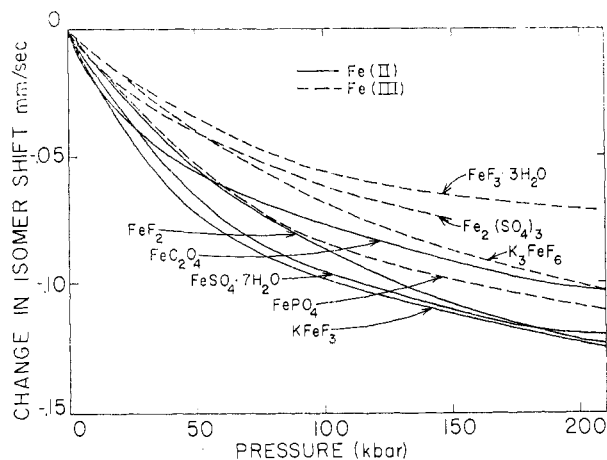


Figure 2. Change of isomer shift *vs.* pressure diagram for "ionic" compounds.

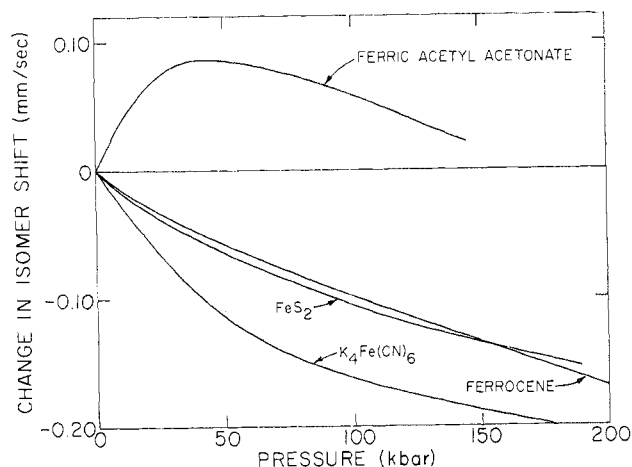


Figure 3. Change of isomer shift *vs.* pressure diagram for "covalent" compounds.

$\alpha$  (or  $\Delta R/R$ ). Walker, *et al.*,<sup>15</sup> have assumed that the configurations of Fe(II) and Fe(III) are  $3d^64s^0$  and  $3d^54s^0$  and have used the difference in measured isomer shift ( $\sim 0.9$  mm/sec) as a scaling factor. On this argument, one would explain the effect of pressure entirely by reduced shielding because the 3d orbitals have spread out, as discussed earlier. This explanation was used by Champion, *et al.*<sup>11</sup> On the other hand, Simanek and Sroubec<sup>16</sup> assume that compression of the wave functions is the major factor in the pressure effect and use the pressure data to evaluate  $\alpha$ , obtaining a number about one-fourth the magnitude of that derived by Walker, *et al.* Gol'danski<sup>17</sup> and Danon<sup>18</sup> arrive at values similar to that of Simanek and Sroubec on more intuitive grounds. Simanek and Sroubec would assign the difference between Fe(II) and Fe(III) isomer shifts

entirely to fractional occupation of the 4s level in the latter case.

Insofar as we can estimate, neither effect is insignificant. There are several factors which make us believe that the change in shielding is more important. (1) Both the range of atmospheric isomer shifts and the range of changes with pressure are quite small. These include ligands with many different propensities for electron sharing. If occupation of the 4s levels were an important factor, one would expect a large spread in isomer shifts. In fact, it is difficult to reconcile the small spread of isomer shifts observed with the results of molecular orbital (LCAO) calculations which indicate a high covalency for Fe(III) which varies widely with the ligand. Apparently this type of wave function is adequate for calculating energy differences observed optically, but is a poor approximation to the amplitude of the ground state as seen at the nucleus. As mentioned earlier, changes in the tail of the wave function are not necessarily reflected in the shape of the inner part. (2) The change in isomer shift with pressure does not correlate with the compressibilities, as would be expected from compression of the s electronic wave functions, but ferrous materials do tend to show a somewhat larger shift than the ferric materials, which would be expected if the dominant mechanism were changing of the 3d shielding. (3) Band calculations for iron<sup>19</sup> indicate that with decreasing interatomic distance the energy of the 3d part of the conduction band lowers in energy *vis-à-vis* the 4s part. Measurements of the change of isomer shift with pressure<sup>3,20-22</sup> combined with the analysis of Ingalls<sup>10</sup> are more consistent with a large negative value of  $\alpha$  as predicted by Walker, *et al.*, than with the smaller magnitude calculated by Simanek and Sroubec. One can relate this to the dominant role of changing 3d shielding. We wish to emphasize, however, that the change of isomer shift with environment is still an open question, and an interesting one.

### The Oxidation State of Iron

As discussed in the previous sections, the Mössbauer spectra of high-spin Fe(II) and Fe(III) are entirely different as regards both isomer shift and quadrupole splitting, so that it is easy to estimate the relative amount of one oxidation state in the presence of the other from computer-fit areas. Although the difference in spectra for low-spin states is less spectacular, the calculation is still possible. One of the most interesting results of high-pressure studies is the observation that ferric ion reduces to the ferrous state with pressure, and this is reversible, with some hysteresis.<sup>9,11-13</sup> Typical spectra appear in ref 9 and 11. A greater or lesser degree of conversion has been observed in  $\text{FeCl}_3$ ,  $\text{FeBr}_3$ ,  $\text{KFeCl}_4$ ,  $\text{Li}_3\text{FeF}_6$ ,  $\text{FePO}_4$ ,  $\text{Fe}_2(\text{SO}_4)_3$ ,  $\text{Fe}(\text{NCS})_3$ ,  $\text{Fe}$ -

(15) L. R. Walker, G. K. Wertheim, and V. Jaccarino, *Phys. Rev.*, **6**, 98 (1961).

(16) E. Simanek and Z. Sroubec, *ibid.*, **163**, 275 (1967).

(17) V. I. Gol'danski, "Proceedings of the Dubna Conference on the Mössbauer Effect," Consultants Bureau Enterprises, New York, N. Y., 1963.

(18) J. Danon, "Application of the Mössbauer Effect in Chemistry and Solid State Physics," International Atomic Energy Commission, Vienna, 1966.

(19) F. Stern, Ph.D. Thesis, Princeton University, 1955 (unpublished).

(20) R. V. Pound, G. B. Benedek, and R. Drever, *Phys. Rev. Letters*, **7**, 465 (1961).

(21) M. Nicol and G. Jura, *Science*, **141**, 1035 (1963).

(22) J. A. Moyzis and H. G. Driekamer, *Phys. Rev.*, in press.

**Table I**  
 Constants for the Equation  $K = C_{II}/C_{III} = AP^B$

Compound	A	B
FeCl <sub>3</sub>	0.265	0.56
FeBr <sub>3</sub>	0.076	0.43
KFeCl <sub>4</sub>	0.092	0.50
FePO <sub>4</sub>	0.078	0.46
Phosphate glass	0.048	0.31
Ferric acetate (418°K)	0.022	0.98
Ferric citrate	0.112	0.25
K <sub>3</sub> Fe(CN) <sub>6</sub>	0.109	2.06

(NH<sub>3</sub>)<sub>6</sub>Cl<sub>3</sub>, K<sub>3</sub>Fe(CN)<sub>6</sub>, ferric citrate, basic ferric acetate, ferric acetylacetonate, ferric oxalate, various hydrates, hemin, and hematin.

The pressure dependence of the conversion is of the form

$$K = AP^B \quad (2)$$

where the equilibrium constant  $K$  is defined as  $K = C_{II}/C_{III}$ , and  $A$  and  $B$  are independent of pressure. Typical values for these constants appear in Table I, and plots are given in Figures 4 and 5 for representative compounds.

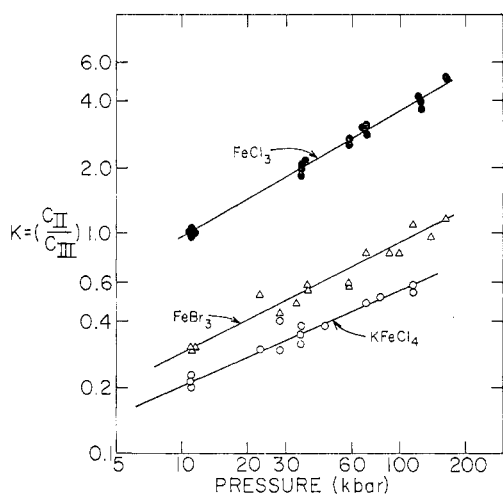


Figure 4.  $\ln K$  vs.  $\ln P$  diagram for halides.

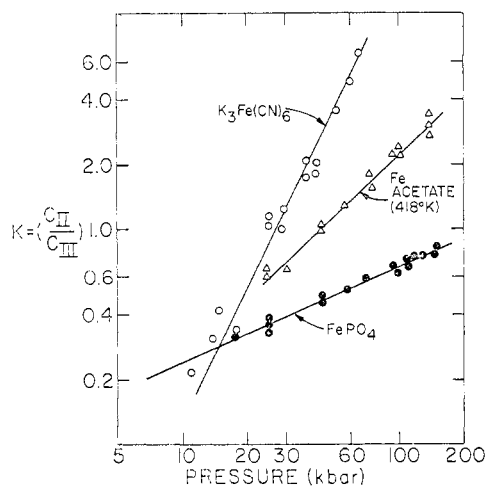


Figure 5.  $\ln K$  vs.  $\ln P$  diagram for FePO<sub>4</sub>, K<sub>3</sub>Fe(CN)<sub>6</sub>, and basic ferric acetate.

Successive spectra at the same pressure are essentially identical, while, after the pressure is changed, as soon as a spectrum is identifiable on the oscilloscope the changed conversion is evident, so it is clear that one is observing equilibrium, not the results of slow kinetics. As discussed in the papers, the concentrations measured are nominal, because of differences in  $\langle x_2 \rangle$  at different sites, etc., but should be a good approximation.

For all compounds studied so far, except hemin and hematin,  $K$  increases with increasing temperature, *i.e.*, the reaction is endothermic,<sup>9</sup> with a heat of reaction in the range 0.1–0.5 eV which usually increases with increasing temperature. For the halides it is independent of pressure but in more covalent systems it may increase or decrease markedly with pressure.

The problems which arise are (1) why there is such a general tendency for ligand-metal electron transfer, and (2) why the pressure dependence is of the observed form, *i.e.*, why there is not a discontinuous reduction at some pressure?

As discussed in the introduction, optical transfer of an electron requires 3–5 eV. The red shift with pressure, while considerable, is not sufficient to move the optical transition to zero energy. However, the high-pressure transition observed here is a thermal effect occurring sufficiently slowly so that the coordinates can assume their new equilibrium values, whereas the optical transition must take place vertically on a configuration coordinate diagram, according to the Franck-Condon principle. The situation is illustrated schematically in Figure 6. The horizontal coordinate is typically displacement along some vibrational mode of the system (metal plus ligands) which permits the rearrangement.

The pressure dependence can be discussed as follows. When electron transfer takes place one creates a ferrous ion in a ferric site plus a radical or radical ion or possibly an excitation smeared out over several ligands. There is, thus, a charge redistribution and local compression and distortion which affect neighboring ions, distorting the potential wells so as to make electron transfer less favorable. Increased pressure lowers the excited state further, allowing more conversion which increases the strain. The hysteresis on release of pressure can be associated with stored-up strain.

A thermodynamic analysis of the situation is given by

$$K = \exp(-G/RT) \quad (3)$$

$$\frac{\partial \ln K}{\partial \ln P} = \frac{P\Delta V}{RT} = \frac{P(V^{III} - V^{II})}{RT} = B \quad (4)$$

eq 3 and 4, where  $V^{III}$  and  $V^{II}$  refer to the volumes of the sites plus their associated ligands. One can rearrange eq 4 to give eq 5. Thus the fractional increase

$$\frac{\partial \ln C_{II}}{\partial \ln P} = P \frac{(V^{III} - V^{II})}{RT} (C_{III}) \quad (5)$$

in conversion with fractional increase in pressure is proportional to the concentration of sites available to convert. The proportionality constant is the work to create a reduced site measured in thermal units (units of

O = OPTICAL TRANSITION  
T ■ THERMAL TRANSITION

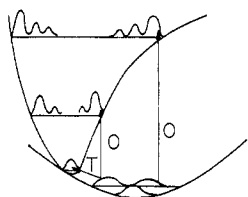


Figure 6. Schematic configuration coordinate diagram.

$RT$ ). The fact that the work is constant is surprising. From our results, it apparently applies in the pressure range 10–200 kbars. Since concentrations below 6–7% or much above 90% are very hard to measure accurately, this relationship may not be valid for dilute mixtures.

The fact that the heat of reaction varies with temperature is reasonable since possible thermal processes include promotion of electrons from ground to excited electronic state, redistribution of electrons among vibrational levels of the ground state, and possible deformation of the potential wells to retard or promote electron transfer.

### Ferrocene

Ferrocene (dicyclopentadienyliron) represents an appropriate material to discuss in detail as its high molecular symmetry,  $D_{5h}$ , has made feasible a number of theoretical studies.<sup>23–27</sup>

Using the SCF-LCAO calculation of Dahl and Ballhausen<sup>27</sup> as a starting point one can account for the pressure-induced effects through ideas developed by Wolfsberg and Helmholz<sup>28</sup> by means of a zeroth order molecular orbital treatment.<sup>29</sup> Wolfsberg and Helmholz made the suggestion that in LCAO molecular orbital treatments the off-diagonal matrix elements could be treated as proportional to the overlap of the corresponding orbitals. In the case of ferrocene, one can obtain the initial matrix elements from the work of Dahl and Ballhausen and one only needs the change that will occur in each matrix element with the reduction in interatomic distance that is produced with the application of pressure. This is obtained in the spirit of the Wolfsberg and Helmholz approximation by assuming that the change produced by pressure in each matrix element is proportional to the change produced in the corresponding overlap integrals.

The precise effect of pressure on the interatomic distances in ferrocene is not known, but an estimate was

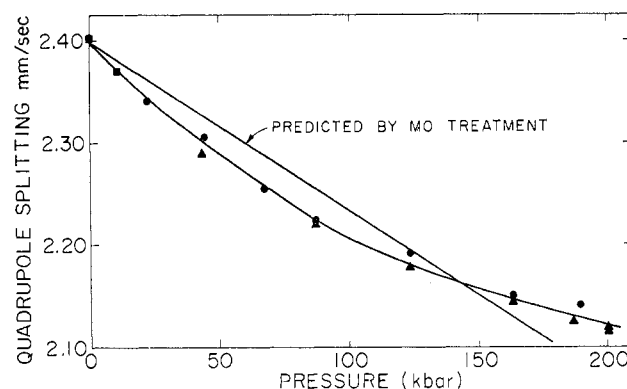


Figure 7. Quadrupole splitting vs. pressure diagram for ferrocene.

obtained from force constants calculated from infrared and Raman spectra. Other high-pressure work<sup>30</sup> has shown the compressibility of the carbon-carbon bond to be small, and as the interest here is in metal-ligand interactions only the carbon-metal distance was assumed to change with pressure. From the published frequencies for the  $A_{1g}$  and  $A_{2u}$  ring-metal stretching frequencies,<sup>31</sup> a compression of about 1% in 100 kbars was predicted.

With this information the necessary overlap integrals were calculated, the off-diagonal elements were adjusted for the change produced in the overlap integrals, and the matrix equations were solved to give the changes in the orbital energies and coefficients of the linear combinations of atomic orbitals.<sup>29</sup> The changes in the electronic parameters considered here, the isomer shift, the quadrupole splitting, and the shift of the optical-absorption peak near  $24,000\text{ cm}^{-1}$  were then extracted from these results.

First, consider the quadrupole splitting. Working within the SCF-LCAO molecular orbital description of Höfflinger and Voitländer,<sup>32</sup> who have examined in detail the various components of the electric-field gradient in ferrocene, and using the necessary numerical constants from their work and the calculated changes in orbital occupation with pressure, the predicted fractional change in the electric field gradient was obtained. The electric field gradient is proportional to the quadrupole splitting, and so the fractional change in the electric field gradient is plotted in Figure 7 as the fractional change in the quadrupole splitting.

The major effect comes from the change in the occupation of the d orbitals. The reduction in the ring-metal distance causes a significant flow of electrons in the  $e_{2g}$  orbitals from metal ( $3d \pm 2$ ) to ligand, and in the  $e_{1g}$  orbitals from ligand to metal ( $3d \pm 1$ ). As the electric-field gradient produced by the  $e_{2g}$  is opposite in sign to that produced by the  $e_{1g}$  orbitals, both contributions add to produce the large decrease in the quadrupole splitting experimentally observed.

(30) R. W. Lynch and H. G. Drickamer, *ibid.*, **44**, 181 (1966).

(31) H. P. Fritz, *Advan. Organometal. Chem.*, **1**, 267 (1964).

(32) V. B. Höfflinger and Voitländer, *Z. Naturforsch.*, **18a**, 1065 (1963); **18a**, 1074 (1963).

(23) R. D. Fisher, *Theor. Chim. Acta*, **1**, 418 (1963).

(24) M. Yamazaki, *J. Chem. Phys.*, **24**, 1260 (1956).

(25) E. M. Shustorovich and M. E. Dayatkina, *Dokl. Akad. Nauk SSSR*, **128**, 1234 (1959).

(26) R. D. Fischer, *Theor. Chim. Acta*, **1**, 418 (1963).

(27) J. P. Dahl and C. J. Ballhausen, *Kgl. Danske Videnskab. Selskab, Mat. Fys. Medd.*, **33**, 39 (1961).

(28) R. W. Vaughan and H. G. Drickamer, *J. Chem. Phys.*, **47**, 468 (1967).

(29) M. Wolfsberg and L. Helmholz, *ibid.*, **20**, 837 (1952).

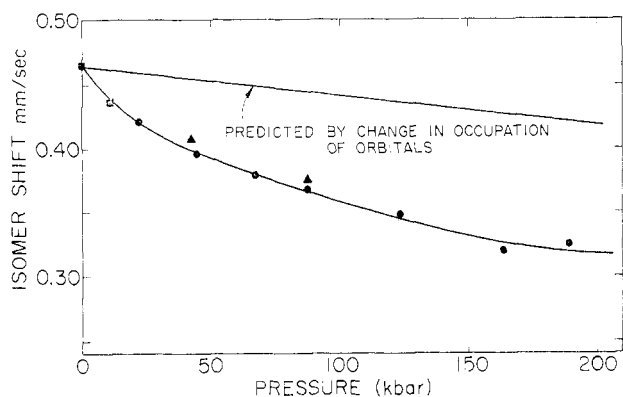


Figure 8. Isomer shift vs. pressure diagram for ferrocene.

The change in the isomer shift with pressure can result from changes in orbital occupation or distortion of the wave function, as discussed above. There is a negligible change in occupation of the 4s orbital predicted, and only a small net decrease in 3d occupation.<sup>29</sup> Using the Walker, *et al.*, calibration<sup>15</sup> for the effect of the change in 3d shielding, the predicted change in the isomer shift due to change in orbital occupation is plotted in Figure 8. This accounts for only a portion of the experimental shift. The SCF-LCAO treatment does not, however, lend itself to a consideration of the orbital distortion effects. This mechanism would be expected to predict an increase in s electron density (as is discussed elsewhere in this paper) and improve the agreement with experiment.

Zahner and Drickamer<sup>33</sup> have reported the shift in the optical absorption peak near 24,000  $\text{cm}^{-1}$  with pressure in ferrocene. This transition is attributed to the  $e_{2g} \rightarrow e^*_{2g}$  ( $A_{2g}$ ) transition by Dahl and Ballhausen, and the effect of pressure on this transition can be obtained from the shift in the  $e_{2g}$  and  $e^*_{2g}$  orbital energies.<sup>29</sup> This is plotted along with the Zahner and Drickamer data in Figure 9.

Thus, an approximate molecular orbital treatment predicts the proper direction and order of magnitude of the pressure-induced shifts in all parameters of the electronic distribution of ferrocene for which experimental data exist. The agreement between theory and experiment is in some cases much better than the approximation made would indicate, and is probably in part fortuitous.

### $\alpha\text{-Fe}_2\text{O}_3$

The Mössbauer effect allows one to follow pressure-induced changes in both the magnetic configuration and local environment in  $\alpha\text{-Fe}_2\text{O}_3$ .<sup>34</sup>

There is a large internal magnetic field present in  $\alpha\text{-Fe}_2\text{O}_3$  due to the antiferromagnetic spin arrangement and there are, therefore, both magnetic dipolar and electric quadrupolar effects present in the Mössbauer spectra. The electric field gradient is axially symmetric,

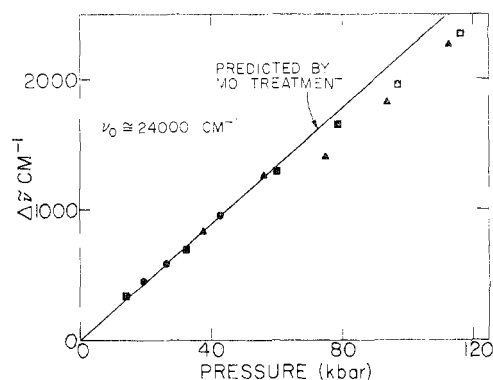


Figure 9. Shift of optical absorption peak vs. pressure diagram for ferrocene.

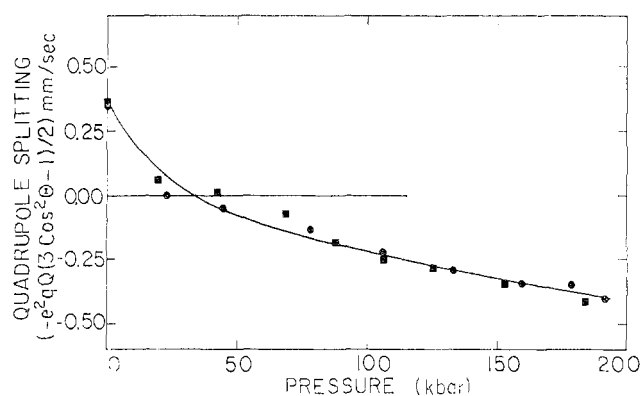


Figure 10. Quadrupole splitting vs. pressure diagram for  $\alpha\text{-Fe}_2\text{O}_3$ .

and the electric quadrupole interaction is much smaller than the magnetic dipole interaction. In this special case the shift of the nuclear energy levels by the simultaneous existence of both interactions is<sup>2</sup>

$$\Delta\epsilon = -g\mu_n H m_I + (-1)^{m_I + 1/2} [1/8 e^2 q Q (3 \cos^2 \theta - 1)]$$

The second term, which represents the effect of the quadrupole interaction, contains an angular factor,  $(3 \cos^2 \theta - 1)$ , where  $\theta$  is the angle between the direction of the magnetic field and the symmetry axis of the electric field gradient. This orientation factor becomes particularly important in the case of  $\alpha\text{-Fe}_2\text{O}_3$  because there is a change in the antiferromagnetic orientation, and thus a change in the direction of the internal magnetic field, near 260°K<sup>35</sup> at 1 atm. From the antiferromagnetic Néel temperature, near 950°K, to about 260°K the direction of the internal magnetic field is perpendicular to the (111) or body diagonal of the rhombohedral unit cell, while at the transition temperature the internal magnetic field rotates 90°, and below this temperature it is parallel to the (111) or body diagonal. As the symmetry axis of the electric-field gradient is along the (111), the angular factor in the above equation,  $(3 \cos^2 \theta - 1)$ , changes from  $-1$  to  $+2$  in going through the transition. This produces a marked effect on the quadrupole splitting when the sample is

(33) J. C. Zahner and H. G. Drickamer, *J. Chem. Phys.*, **35**, 375 (1961).

(34) R. W. Vaughan and H. G. Drickamer, *ibid.*, **47**, 1530 (1967).

(35) C. G. Shull, W. A. Strauser, and E. O. Wollan, *Phys. Rev.*, **83**, 333 (1951).

cooled through the transition temperature. Ôno and Ito<sup>36</sup> reported a broadening of the Mössbauer peaks as the transition temperature was reached due to the simultaneous existence of both antiferromagnetic phases and the predicted change in sign and doubling in magnitude of the quadrupole splitting.

The effect of pressure on the quadrupole splitting is shown in Figure 10; the splitting passes through zero near 30 kbars, changes sign, and then grows with increasing pressure to about the original magnitude by 200 kbars. Measurements have indicated that the temperature of the Morin transition does increase with pressure,<sup>37,38</sup> and Worlton, *et al.*,<sup>39</sup> have recently reported that it reaches room temperature near 30 kbars. This agrees well with the point where the quadrupole splitting goes through zero, but if the explanation of the quadrupole splitting data were simply the occurrence of the Morin transition with increasing pressure, the peak broadening reported by Ôno and Ito should be detectable and the observed quadrupole splitting should have grown to nearly twice the original size.

(36) K. Ôno and A. Ito, *J. Phys. Soc. Japan*, **17**, 1012 (1962).

(37) R. C. Wayne and D. H. Anderson, *Phys. Rev.*, **155**, 496 (1967).

(38) H. Umehayoshi, B. C. Frayer, G. Shirane, and W. B. Daniels, *Phys. Letters*, **22**, 407 (1966).

(39) T. G. Worlton, R. B. Bennion, and R. M. Brugger, *ibid.*, **A24**, 653 (1967).

The absence of these phenomena indicates that a reduction has occurred in the electric-field gradient before or during the Morin transition. One can interpret this reduction in the electric-field gradient in terms of local movement of ions within the unit cell using a point dipole model for the  $\alpha$ -Fe<sub>2</sub>O<sub>3</sub> structure. A calculation of this effect<sup>34</sup> indicates that a movement of the iron ion of only 0.04 Å along the body diagonal of the rhombohedral unit cell is sufficient to account for the abnormalities noted in the Mössbauer spectra.

Worlton and Decker<sup>40</sup> have, however, shown that these Mössbauer results, as well as neutron diffraction studies to 40 kbars, can be more plausibly explained by assuming a continuous change in the angle of the antiferromagnetic axis with respect to the (111) axis of the crystal with increasing pressure.

This relatively brief presentation illustrates the power of high-pressure Mössbauer resonance as a tool for uncovering new generalizations about electronic behavior in solids as well as for investigating the electronic structure of specific systems.

*The authors express their appreciation to C. P. Slichter, G. K. Lewis, Jr., S. C. Fung, and W. H. Flygare for very helpful discussions and collaboration in many aspects of this work.*

(40) T. G. Worlton and D. L. Decker, *Phys. Rev.*, **171**, 596 (1968).

## Purine 8-Cyclonucleosides

MORIO IKEHARA

*Faculty of Pharmaceutical Sciences, Osaka University, Toyonaka, Osaka, Japan*

*Received July 12, 1968*

Although nucleosides, as essential components of nucleic acids, have been widely studied, the somewhat more elaborate *cyclonucleosides* have received relatively little attention. The first cyclonucleoside was discovered by Lord Todd and his colleagues in 1951.<sup>1</sup> Subsequently, these compounds have become of interest in connection with nucleoside configurational studies. Also, their rigid structures facilitate interpretation of physical properties with respect to structural characteristics, and they are key intermediates in the synthesis of many biologically active substances. Their synthesis has been a considerable challenge in its own right.

To date, no cyclonucleoside has been found to occur naturally, either free or in bound form.

A few words about nomenclature are in order. Certain purine and pyrimidine bases are prominent in the

biochemistry of nucleic acids in which these bases are covalently bound to sugar residues, either ribose or 2-deoxyribose, *via* glycosidic linkages. Compounds having one purine or pyrimidine base bound to one sugar residue are called *nucleosides*. For example, guanosine (**1**) is a nucleoside containing guanine and ribose moieties, and thymidine (**2**) contains thymine and 2-deoxyribose moieties. *Nucleotides* are phosphoric acid esters of nucleosides, at the 2', 3', or 5' positions. Thus, in a nucleotide, the 5' substituent may be OPO<sub>3</sub>H<sub>2</sub> instead of OH as in the nucleoside. *Nucleic acids* are polymeric, and can be thought to represent esterification, many times repeated, between the 3'-hydroxyl group of one nucleotide molecule and the 5'-PPO<sub>3</sub>H<sub>2</sub> group of another. *Cyclonucleosides* differ from ordinary nucleosides in that they have a covalent linkage, either directly or *via* bridging oxygen atoms, etc., between the 2', 3', or 5' carbon of the sugar moiety and a carbon or nitrogen atom of the purine or pyrimidine moiety (other than the nitrogen

(1) V. M. Clark, A. R. Todd, and J. Zussman, *J. Chem. Soc.*, 2952 (1951).